Structural role of titanium on slag properties

Domitille Le Cornec, Laurence Galoisy, Laurent Izoret, Laurent Cormier, Nicolas Trcera, Georges Calas

Structural role of titanium on slag properties

Domitille Le Cornec[1,a,b], Laurence Galoisy[a,*], Laurent Izoret[b], Laurent Cormier[a], Nicolas Trcera[c], Georges Calas[a]

[a] *Sorbonne Université, Muséum National d'Histoire Naturelle, CNRS, Institut de Minéralogie, de Physique des Matériaux et de Cosmochimie, IMPMC, 75005 Paris, France*

laurence.galoisy@sorbonne-universite.fr; laurent.cormier@sorbonne-universite.fr; georges.calas@sorbonne-universite.fr; domitille.le-cornec@espci.fr

[b] *Association Technique de l'Industrie des Liants Hydrauliques (ATILH), 7 place de la Défense, 92974 Paris-La-Défense Cedex, France*

l.izoret@atilh.fr

[c] *Synchrotron SOLEIL, L'Orme des Merisiers, Saint Aubin BP48, 91192 Gif sur Yvette cedex, France*

nicolas.trcera@synchrotron-soleil.fr

Keywords

Slags; Glass; Titanium oxide; Electron Spin Resonance (ESR); Atomic structure; XANES

[1] *Present Address: Saint-Gobain Recherche, Paris 39 quai Lefranc 93303 Aubervilliers cedex, France*

**corresponding author : Laurence Galoisy, Sorbonne Université, IMPMC, BC 115, 4 place Jussieu 75005 Paris, France*

Abstract

The presence of titanium in Ground Granulated Blast-furnace Slags (GGBS) has been suspected to modify cement properties. This study provides the first evidence of a relation between the TiO_2 content of slags and the mechanical properties of mortars based on slag cements. It is observed that only the slags containing less than 1%TiO_2 show a compressive strength at 28 days that remains within the 52.5 MPa norm with CEM III cements complying with the European Standard NF EN 197-1. The structural origin of this chemical dependence of the performance of cements is investigated by determining directly the titanium speciation in various European slags by spectroscopic methods. Electron Paramagnetic Resonance indicates that about 76% of Ti in slag occurs as Ti^{4+}. The atomic structure around Ti was determined by Ti K-edge X-ray Absorption Near Edge Spectroscopy, which shows that Ti is mainly 5-fold coordinated in square-based pyramid geometry. Five coordinated Ti acts as network-stabilizer of the silicate network as it increases the polymerization. Requiring Ca^{2+} for charge-compensation of the titanyl bond, it reduces the availability of Ca^{2+} during glass alteration in a modified random model of glass structure, where Ca^{2+} atoms are clustered in percolating cationic domains. As a consequence, the presence of 5-coordinated Ti results in a slower dissolution of the slag. These peculiar structural properties of titanium may explain the detrimental role of Ti above a 1% concentration, for many physical and chemical slag properties. This work provides a scientific ground for the technological acceptability of the upper limit of the Ti-content of GGBS.

1. Introduction

Portland cement is the dominant binder used in concrete for construction with an annual worldwide production exceeding now 4 Gt/year,[1] accounting for about 2% of the global primary energy consumption and 5% of anthropogenic CO_2 emissions.[2] Within the scope of a circular economy imposed by the future scarcity of primary raw materials,[3] the waste produced by other industries may be used as low-CO_2 binders.[4] Among these secondary raw materials, Ground Granulated Blast-furnace Slags (GGBS) from steelmaking industry can be used as supplementary cementitious materials (SCM) for producing low carbon footprint cements ("green cements"). GGBS is an amorphous by-product obtained by rapid cooling under water of high temperature molten silicate slags. It has been used as SCM for about a century due to its latent hydraulic properties. In addition to reducing the environmental footprint of cement by limiting the use of

clinker,[5] the use of GGBS improves the durability of concrete. For instance, the replacement of Portland cement by GGBS increases the resistance of concrete and mortar against chloride penetration and sodium sulfate attack, with insignificant mass transfers between mortar and solution.[6,7] Ground granulated blast-furnace slags are calcium aluminosilicate glasses, which contain a dozen oxides including TiO_2.[8] "Green" cements can be made with up to 95% GGBS. However, their implementation remains challenging, as the use of GGBS represents a substantial departure from the traditional chemistry of Portland cement. In particular, modeling the reactivity of the slag in water when mixed with clinker requires a better understanding of the influence of slag processing and physicochemical properties on their performance. Various parameters have been linked to the reactivity of GGBS such as the glass content, the particle size distribution and the chemical composition of the slag.[9] As underlined recently, it is clear that a lower polymerization of the amorphous network leads to a higher reactivity.[10] Among the components of GGBS, the CaO/ SiO_2 ratio and the Al_2O_3 and TiO_2 contents can exert a substantial influence on glass reactivity.[11] Despite various quality parameters, that may be used to predict slag reactivity, as briefly discussed in Section 2.1, a quantitative evaluation of slag and SCMs reactivity is still an important issue (see e.g. RILEM TC 267 TRM). As the chemical composition of the slag plays a key role in slag reactivity,[12] a better understanding of the atomic structure of GGBS may help assess their hydration properties.

2. Technological context

Among the minor components of slags, TiO_2 has a peculiar origin. It is contained in the raw materials used for steelmaking, but it can be also intentionally added as ilmenite ($FeTiO_3$). Indeed, the presence of titanium during steelmaking helps protect the refractory materials of the blast furnace and extends its lifetime. Titanium can be present in slags as Ti^{4+} and Ti^{3+}, as the molten slag is formed in a blast-furnace under reducing conditions that favor the presence of some Ti as Ti^{3+},[13] as shown in titania slags.[14] Even at low TiO_2 contents, the presence of Ti leads to changes in the structure of the amorphous slags.[9,15] The increase of slag density at higher Ti-content has been related to the presence of high coordinated Ti.[9] Also, with increasing amounts of TiO_2, the corrosion resistance and the porosity of the GGBS increase.[9,13,16] All these slag properties generally change at a limit of about 1 % TiO_2,[9,17,18] even if the exact value of this limit differs depending on the blast furnace slag considered.

The incidence of Ti on the mechanical properties of mortars and concretes elaborated with GGBS is a concern. It has been observed that the early strength of GGBS-based mortars may be

reduced if the TiO_2 content exceeds 1%:[17] a higher TiO_2 concentration induces a loss of reactivity of slag cement in water and a drop of the early compressive strength of the associated mortar that is no longer acceptable from the point of view of industrial norms.[9,15,18,19] An inverse correlation between TiO_2 concentration and the mechanical strength of mortars may also be observed for TiO_2 contents smaller than 1%: Figure 1 shows the performance of GGBS-based mortars, monitored by the mechanical strength at 28 days of standard mortar test specimens, following the norm NF EN 196-1 on samples (40 x 40 x160 mm). A linear regression analysis indicates a correlation coefficient R equal to 0.86 (42 samples) and 0.93 (8 samples) for cements containing 60% and 70% slag, respectively. This inverse correlation suggests a loss of short-term reactivity of the slag as its titanium content increases. However, this variation remains acceptable as far as the compressive strength at 28 days remains within the norm, i.e. 52.5 MPa at 28 days for CEM III cements complying with European Standard NF EN 197-1. Figure 1 shows that, though titanium concentration remains low, the modification of the mechanical resistance is about 5 and 15 MPa for cements containing 60% and 70% slag, respectively. This is a high variation by comparison with the standard deviation on the overall industrial production of cements CEM III / A and B, which remains of the order of 1.5 - 1.8 MPa after 28 days.[9] It is of interest that the 52.5 MPa limit of the NF EN 197- 1 Standard corresponds to a 1% TiO_2 content of the slags, for cements containing 60% slag, as shown on Figure 1.

The present study aims to assess, based on spectroscopic data, the speciation of Ti, i.e., its oxidation state and coordination number in the atomic structure of GGBS with a TiO_2 content below or around the specification range of 1% TiO_2. Electron paramagnetic resonance (EPR) and Ti K-edge X-ray absorption near-edge spectroscopy (XANES) show that titanium, mainly as Ti^{4+}, occurs in 5-coordination (square- based pyramid) in all slags investigated. This peculiar geometry of the Ti-site influences the local polymerization. It may account for the adverse role of Ti on physical and chemical properties of GGBS, including its influence on the mechanical resistance of GGBS-based mortars at 28 days.

3. Experimental

3.1. Materials

Six representative GGBS were selected from various European cement plants. Table 1 gives an overview of their chemical composition obtained by X-ray fluorescence analysis. Their amorphous nature is confirmed by x-ray diffraction (Figure S1) and optical isotropy.

According to various parameters aimed to estimate the reactivity and solubility of GGBS, these slags are within the EN 15167-1 European standard or in accordance with values currently used in the industrial practice. These slags match the common acceptance criteria:[12]

- The basicity indices, C/S, C+M/S and (C+M)/(S+A), are larger than 1.
- The glass forming index, C+M+S, is higher than 66%.

The hydraulic indices are given by relations predicting the slag performance in terms of hydraulic reactivity, such as the Tetmayer modulus and the Hydraulic index, and are also satisfied, as they are simultaneously higher than 1.

Slags 2 and 5 were also remelted at 1400°C for 1h in air in a platinum crucible. The melts were quenched by immersion of the bottom of the platinum crucible in water avoiding any contact between water and the remelted slag. All samples were ground in an agate mortar.

3.2. EPR measurements

An assessment of the Ti^{3+} content of the samples was made by electron paramagnetic resonance (EPR). EPR spectra were recorded at X-band (9.4 GHz) and 1 mW microwave power, using a Bruker EMXplus spectrometer. The measurements were performed at low temperature (90 K, i.e. about -183 °C) to maximize the intensity of the signal. A 2,2-diphenyl-1-picrylhydrazyl (DPPH) reference sample was used to calibrate the magnetic field. The intensity of the spectra was normalized by the weight of the sample, the receiver gain, a filling factor depending on the height of the sample in the tube and resulting from the non-uniformity of the magnetic field in the resonator and the modulation amplitude.[20] The concentration of the paramagnetic species was calculated by reference to an alanine reference sample (Bruker ER213ASC) with a known concentration of 1.75×10^{17} +/- 10% spins.

3.3. XANES measurements

Ti K-edge X-ray absorption near-edge structure (XANES) spectra of the amorphous slags were recorded in the fluorescence mode on the LUCIA beamline of the SOLEIL synchrotron (Saint-Aubin, France) using a Si(311) monochromator giving a spectral resolution of 0.15 eV. The XANES spectra were all normalized with the same parameters using ATHENA software.[21] The intensity and energy position of the pre-edge features were determined by fitting the corresponding peak with a Lorentzian function after removal of an arctangent background. The accuracy of the

extracted pre-edge intensity is 0.03 (a.u.). The crystalline references for XANES spectroscopy were rutile (TiO_2) and fresnoite ($Ba_2TiSi_2O_8$) for $^{[6]}$Ti and $^{[5]}$Ti, respectively. A $K_2O.TiO_2.2\ SiO_2$ (KTS2) glass was also used for comparison as it only contains $^{[5]}$Ti.[22]

3. Results

3.1. EPR

The redox state of Ti cannot be quantified chemically in slags, due to the presence of other redox- sensitive elements (Fe, Mn). However, EPR spectra can be used to determine the concentration of paramagnetic species that may correspond to some oxidation states of transition elements (e.g. Ti^{3+}, Fe^{3+}, Mn^{2+}...). The EPR spectra of the slags present a resonance near 3500G (Figure 2). This signal is broad and asymmetric and is assigned to Ti^{3+} (Figure S2).[23] This asymmetry indicates that Ti^{3+} occurs in a distorted site. Moreover, the Ti^{3+} signal is superimposed by a broad signal due to the presence of magnetic clusters, which may indicate minor amounts of a RO phase (FeO–MgO–MnO–CaO solid solution) often found in slags.[24] There is no signal due to isolated Fe^{3+} in the amorphous matrix, showing that all Fe is in the divalent state, as a consequence of the reducing conditions during steelmaking in the blast furnace. In order to better constrain the speciation of Ti and Fe, the slags were remelted under oxidizing conditions. In these remelted slags, the Ti^{3+} signal disappears (Figure 2), showing that all Ti^{3+} is oxidized to Ti^{4+}. At the same time, an intense Fe^{3+} resonance appears near 800 and 1500G, which results from the partial oxidation of Fe^{2+} during remelting in air. It is noteworthy that the broad signal assigned to the RO phase around 2500G is not affected by slag melting under oxidizing conditions.

Under the assumption of a proportional evolution of the Ti^{3+} content with the total Ti content, a Ti^{4+}/Ti(total) ratio of 76% (+/-7.2%) can be estimated from the slope of a linear regression of the Ti^{3+} EPR data on the investigated slags (Figure S3). The high reliability of the linear regression analysis demonstrates that the oxidation state of titanium is similar in all samples investigated.

3.2. Ti K-edge XANES

XANES allows determining the coordination number of Ti ($^{[4]}$-, $^{[5]}$- and $^{[6]}$Ti). The low-energy side of the absorption edge (Figure 3) corresponds to the pre-edge, which is a specific feature, the intensity of which is enhanced for $^{[4]}$Ti and $^{[5]}$Ti sites, as compared to a $^{[6]}$Ti site. The sensitivity of XANES allows investigating the proportion of Ti coordination numbers,[25,26] as shown in Figure 4.

The XANES spectra of slags (Figure 3) present an intense pre-edge feature (labeled A) at 4970 eV and two main features (labeled B and C) located at 4986 eV and 4998 eV. No significant feature appears at higher energy, by contrast to the crystalline references. This arises from the absence of long distance ordering in these amorphous slags. The B and C features are quite similar to those observed on the $K_2O.TiO_2.2\ SiO_2$ (KTS2) reference glass, except for a small shoulder appearing near peak C, at about 5005 eV in KTS2. As KTS2 contains mostly $^{[5]}$Ti, the overall similarity of the XANES data suggests that Ti^{4+} and Ti^{3+} are also dominantly 5-coordinated in slags.

This is confirmed by a detailed examination of the pre-edge. The energy position of this feature is shifted by about 0.5 eV relative to that of $^{[4]}$Ti (Figure 4). The pre-edge shows a similar shape and intensity for all ground slag samples and the $^{[5]}$Ti references, KTS2 and fresnoite ($Ba_2TiOSi_2O_7$). Based on the energy position of this pre-edge and its intensity, Figure 4 indicates that the investigated slags do not contain measurable amounts of $^{[6]}$Ti, Ti being mainly 5-coordinated, with a minor contribution of tetrahedral Ti. The intensity of the pre-edge feature (Figure S4) increases by 10%, without change in the energy position or linewidth, from the pristine slags, which contain Ti^{3+} and Ti^{4+}, to the remelted slags, which contain only Ti^{4+}: this confirms the similar speciation of Ti^{3+} and Ti^{4+}.

4. Discussion

4.1. Speciation of Ti

Titanium occurs in glasses under 3 different coordination numbers: $^{[4]}$Ti, $^{[5]}$Ti, $^{[6]}$Ti. When Ti is 4- coordinated, i.e. in tetrahedral coordination, it may occur in a network-forming position, although its ionic radius is almost twice as large as that of Si (0.42 Å vs. 0.26Å for $^{[4]}Ti^{4+}$ and $^{[4]}Si^{4+}$, respectively). When Ti is 6-coordinated, it is located in octahedral sites, acting as a

network modifier. However, X-ray absorption spectroscopy at K- and L-edge and neutron diffraction studies indicate that Ti is 5-coordinated in most silicate glasses.[22,25, 27] This study shows that it is also the preferred coordination of Ti in all investigated slags. There is no difference between the speciation of titanium in the slags that are inside or outside the specification range of [Ti]<1 %: the local environment of Ti in these aluminosilicate glasses is remarkably constant and is not affected by variations in the Ti-content. This is in line with literature structural data on Ti speciation in Ti-rich slags, based on the model system CaO-Al_2O_3-SiO_2-TiO_2, where a Raman peak near 870 cm^{-1} has been recently assigned to the presence of a $^{[5]}$Ti-O-Si vibration,[28] revising previous interpretations indicating the presence of $^{[4]}$Ti.[29]

Spectroscopic data demonstrate that titanium is present as Ti^{3+} and Ti^{4+} in blast furnace slags, Ti^{4+} being the main oxidation state. The presence of Ti^{3+} is consistent with the reducing conditions of slag formation in blast furnaces. These conditions, intended to reduce the iron ore, are however not reducing enough to reduce all Ti into Ti^{3+}. Ti is mainly 5-fold coordinated under these two oxidation states in the slags. No $^{[6]}Ti^{4+}$ contribution is evidenced by XANES and the absence of $^{[6]}Ti^{3+}$ is confirmed using UV-visible spectroscopy (not presented here) by the absence of a characteristic Ti^{3+} absorption band at 20 000cm^{-1}.[30] These results are consistent with the predominance of $^{[5]}$Ti observed in alkaline-earth silicate glasses with a low TiO_2 content.[27]

The similarity of of the XANES spectra of slags and the reference KTS2 glass indicates that five-fold coordinated Ti occurs in a square-based pyramid with four basal Ti-O bonds of 1.9-2.0 Å and one shorter titanyl bond of 1.65-1.76 Å (Figure 5a).[22,27] This confirms that 5-coordination is a common coordination of transition elements in glasses.[31,32] By contrast to previous assumptions of a change from tetrahedral to octahedral Ti-coordination with increasing Ti content above 1 % in slags,[9] the present study does not show any evidence of a concentration-dependent modification of Ti coordination, Ti remaining in 5-coordination.

4.2. Influence of the speciation of Ti on the structure of amorphous slags

The presence of five-coordinated Ti influences the atomic scale structure at a medium range, with potential consequences on slag properties. With this coordination site geometry, Ti plays a dual role in the amorphous structure of slags. The oxygen of the titanyl bond is non-bridging (i.e. non- bonded to a SiO_4 tetrahedron): this bond gives Ti the role of a network-modifier cation. At the same time, the four basal Ti-O bonds imply oxygen atoms that link the Ti site to the

(Si,Al)O_4 tetrahedra of the aluminosilicate network (Figure 5b): in that case, the bridging oxygen atoms (Ti-O-Si) make Ti play the role of a network-former cation. In this peculiar five-coordination, there is a charge deficit localized on the oxygen of the titanyl bond and the remaining negative charge of the $^{[5]}$Ti square-based pyramid has to be compensated by cations.[22] As $^{[4]}Al^{3+}$ is charge-compensated by Na^+ preferentially to Ca^{2+},[33,34] the few alkalis present in the composition of the slags will preferentially compensate $^{[4]}$Al. Five-coordinated Ti will therefore be compensated only by Ca^{2+}, a peculiar structural property that may be related to the anomalies related to the presence of Ti, as discussed in Section 2.

The Ca^{2+} ions compensating the charge deficit of the underbonded oxygen atom of the titanyl moiety, can no more be considered as network modifiers in the structure of the slag. The amorphous network is therefore more polymerized around $^{[5]}$Ti. As minority Ti^{3+} occurs in a similar site as $^{[5]}Ti^{4+}$, the amorphous network will also be stabilized around $^{[5]}Ti^{3+}$. In addition, the charge-compensating Ca^{2+} cations can be expected to be more difficult to exchange than network-modifiers during the hydration of the amorphous slag. An analogous behavior for Na^+ can be found in sodium aluminosilicate glasses hydrated in water, where the Na^+ ions that play the role of network modifiers are selectively leached, whereas the Na^+ ions charge compensating tetrahedral Al^{3+} remain untouched.[35]

These results are consistent with the correlation between the Ti concentration and an increase of the polymerization stabilizing the silicate network through the Ti-O-Si linkages that imply the four basal oxygen atoms of the square pyramid Ti-site. Such a polymerization with increasing TiO_2 content has been observed by Raman spectroscopy in amorphous slags resulting from the vitrification of air pollution control residue[36] and in CaO-MgO-SiO_2-TiO_2 slags.[28] Under these conditions, the concentration of Si tetrahedra in Q^2 and Q^3 configuration increases while the number of Q^0 and Q^1 species decreases, resulting in a more polymerized amorphous network. This modifies the medium range structural organization of the amorphous slags, because of the heterogeneous structure predicted by the modified random network model of silicate glasses.[37] In this model, $^{[5]}$Ti is located at the interface between the polymeric network (containing SiO_4 and AlO_4 tetrahedra and the bridging oxygen atoms of the TiO_5 sites) and percolating cation-rich domains (containing Ca^{2+} and Na^+ ions and the titanyl oxygens). This picture of the structural role of titanium in glasses is more complex than the previous description based on the coexistence of $^{[4]}$Ti and $^{[6]}$Ti.[9] A model similar to ours accounts for the peculiar properties of Ti-containing aluminosilicate glasses. The presence of titanium decreases the concentration of network

modifying cations leading to the coexistence of two kinds of connected sub-domains: one in which SiO_4 tetrahedra and $^{[5]}Ti$, charge balanced by cations, are linked together, the other based on interconnected SiO_4 and tetrahedral alumina charge balanced by cations.[38]

4.3. Titanium influence on slag reactivity

Low amounts of titanium have long been known to affect physical and chemical properties of glasses and melts.[39] In slags, despite the minor Ti concentration, the presence of this element has been often invoked to explain the modification of several properties, including density, color, porosity, slag reactivity and compressive strength of mortars.[9] For instance, it has been mentioned that the presence of high contents of Ti in slags can lead to an unwanted concrete color, which is actually light when using cement with a high slag content.[9] As shown in Section 2, most studies mention a critical Ti-concentration of about 1 %, above which slag properties are modified. By contrast, a TiO_2 content lower than about 1 % is considered uncritical.[15] More specifically, low amounts of TiO_2 play a detrimental role on the reactivity of a large diversity of oxide glasses of technological interest, even for Ti-concentrations at the 1 % level. The reactivity of Ti-rich slags from the vitrification of air pollution control residues decreases with increasing TiO_2-content, which has been attributed to an increasing polymerization of the amorphous network.[36] In borosilicate glasses of nuclear interest, adding 1 % TiO_2 decreases the initial dissolution rate by a factor of two.[40] Similarly, the addition of 2% TiO_2 to E-glasses enhances the corrosion resistance of glass fibers.[41] A final example concerns phosphate glasses, for which the solubility decreases by 30% over 21 days, as the TiO_2 content increases from 0.2 to 1 %.[42]

The structural origin of the influence of Ti on slag reactivity may be related to the 5-coordination of this element and the subsequent need for charge compensation. Indeed, recent diffraction and Molecular Dynamics/Reverse Monde Carlo numerical simulations studies have demonstrated that the structure of slags is characterized by Ca^{2+} ions occurring preferentially in concentrated domains percolating the silicate network (Figure 5c). Since the ionic bonds are more reactive than the covalent bonds, these percolating domains may be preferential pathways of water molecules during glass alteration[37]. This may explain the influence of low amounts of titanium on slag properties, by breaking the connectivity of these alteration pathways, as Ca mobility during slag corrosion will be locally hindered by the need to charge-compensate the neighboring $^{[5]}Ti$ sites.

The porosity of slags is another property of technological concern. It is related to melt viscosity and the ease to nucleating gas bubbles to escape. The addition of TiO_2 increases the viscosity of aluminosilicate melts, which was found to be consistent with majority $^{[5]}Ti$.[38] In slags, a higher porosity has been observed at a TiO_2 content higher than about 1 %, which may result from a higher viscosity of the liquid blast furnace slag before granulation.[9] The peculiar square-pyramid geometry of 5-coordinated Ti in GGBS slags imposes an increasing polymerization of the silicate network around Ti, through Ti-O-Si linkages. This is at the origin of an increased viscosity of Ti-bearing silicate melts. The increased porosity of TiO_2-rich GGBS facilitates their grindability, but also gives rise to higher residual moisture, which is detrimental and has to be driven out in an energy-intensive manner.[9]

5. Conclusion and perspectives

This study shows a clear inverse relationship between Ti concentration of slags and cement performance, demonstrating the existence of a critical value of 1% TiO_2 below which titanium may be accepted for CEM-III cements to remain within the industrial norm NF EN197- 1. The structural origin of this influence has been directly investigated through chemically selective spectroscopic methods (EPR and Ti K-edge XANES) that allow determine the speciation of Ti in amorphous blast-furnace slags. In all studied slags, the main oxidation state is Ti^{4+}, with about 24 (+/- 7.2) % of the Ti atoms being Ti^{3+}, as shown by EPR. Titanium K-edge XANES shows that Ti is mainly 5-fold coordinated. In this environment, Ti is in square-based pyramid geometry. In this peculiar atomic arrangement, Ti plays a dual role of network-former and network-modifier. The speciation of Ti is the same in all studied slags, including those outside the specification range of about 1 % [TiO_2]. Five-fold coordinated Ti acts as a network-stabilizer as it increases the polymerization of the silicate network through the T-O-Si linkages formed by the oxygen neighbors forming the base of the square pyramid. Simple charge balance arguments suggest that the titanyl bond of the five-fold coordinated Ti requires Ca for charge compensation. This reduces the availability of network-modifiers ions in the glass. This speciation modifies the medium range structural organization of the amorphous slag, which gives a structural ground to the origin of the detrimental role played by titanium in the physical and chemical properties of the slags used as a supplementary cementitious materials at Ti- concentrations as low as 1%. As an outlook, it can be speculated that favoring 4- or 6-fold Ti coordination states -which do not require charge compensation by Ca- may mitigate the penalizing role of Ti in CEM-III cements.

Credit author statement

Domitille Le Cornec: Investigation, Formal analysis, Writing- Original draft preparation, Visualization **Laurence Galoisy:** Project administration, conceptualization, writing-Review and Editing **Laurent Izoret*:*** Supervision, Conceptualization, Funding acquisition, writing-Review and Editing **Laurent Cormier:** writing-Review and Editing, Visualization **Nicolas Trcera:** writing-Review and Editing **Georges Calas*:*** Project administration, writing-Review and Editing, Visualization

Acknowledgments

We thank ATILH (*Association Technique de l'Industrie des Liants Hydrauliques*) for providing us access to their database, allowing us to demonstrate the relationship between titanium concentration and cement performance. The authors want to thank Maxime Guillaumet for his help on EPR measurements and the staff of SOLEIL, and more particularly of the LUCIA beamline, for their help for XANES acquisition. We thank Horacio Colina (ATILH) for fruitful discussions. We acknowledge the continuous support of ATILH (*Association Technique de l'Industrie des Liants Hydrauliques*) for providing slag samples characterized by X-ray fluorescence and the affiliated cement companies for sharing their technological and industrial experience. This work was supported by ATILH and ANRT (*Association Nationale de la Recherche et de la Technologie*), under the CIFRE contract 2016/1343. This manuscript has been improved by the useful comments of the two anonymous reviewers.

References

[1] Andrew, RM, Global CO_2 emissions from cement production, 1928-2018. Earth Syst. Sci. Data 2019;11:1675-1710.https://doi.org/10.5194/essd-11-1675-2019.

[2] International Cement Review, Global Cement Report, 13th ed. 2020.

[3] Calas G. Mineral Resources and Sustainable Development. Elements. 2017;13:301–306. https://doi.org/10.2138/gselements.13.5.301.

[4] Shi C, Qu B, Provis JL. Recent progress in low-carbon binders. Cem. Concr. Res. 2019;122 227– 250. https://doi.org/10.1016/j.cemconres.2019.05.009.

[5] Yang KH, Jung YB, Cho MS, Tae SH. Effect of supplementary cementitious materials on reduction of CO_2 emissions from concrete. J. Clean. Prod. 2015;103:774-783. https://doi.org/10.1016/j.jclepro.2014.03.018.

[6] Ukpata JO, Muhammed Basheer PA, Black L. Expansion of CEM I and slag-blended cement mortars exposed to combined chloride-sulphate environments Cem. Concr. Res. 2019; 123:105794. https://doi.org/10.1016/j.cemconres.2019.105794.

[7] Otieno M, Beushausen H, Alexander M. Effect of chemical composition of slag on chloride penetration

resistance of concrete. Cem. Concr. Compos. 2014; 46:56-64. https://doi.org/10.1016/j.cemconcomp.2013.11.003.

[8] Lothenbach B, Scrivener K, Hooton RD. Supplementary cementitious materials. Cement Concr. Res. 2011; 41:1244–1256. https://doi.org/10.1016/j.cemconres.2010.12.001.

[9] Ehrenberg A. Hüttensand-Ein leistungsfähiger Baustoff mit Tradition und Zukunft-Teil 2, Beton-Informationen. 2006;5:67–95.

[10] Schöeler A, Winnefeld F, Haha MB, Lothenbach B. The effect of glass composition on the reactivity of synthetic glasses. J. Am. Ceram. Soc. 2017; 100:2553–2567. https://doi.org/10.1111/jace.14759.

[11] Tänzer R, Buchwald A, Stephan D. Effect of slag chemistry on the hydration of alkali- activated blast-furnace slag. Mater. Struct. 2015; 48:629–641. https://doi.org/10.1617/s11527-014- 0461-x.

[12] Darquennes A, Espion B, Staquet S. How to assess the hydration of slag cement concretes? Constr. Build. Mater.2013;40:1012-1020. https://doi.org/10.1016/j.conbuildmat.2012.09.087.

[13] Sun J, Wang S, Chu M, et al. Titanium distribution between blast furnace slag and iron for blast furnace linings protection. Ironmak. Steelmak. 2018;1–8. https://doi.org/10.1080/03019233.2018.1557847.

[14] de Villiers J, Balan E, Calas G, Bessinger D, Eeckhout S, Glatzel P. The determination of Ti_2O_3 in titania slags: a comparison of different methods of analysis. Miner. Process. Extr. Metall. 2008; 117:166– 170. https://doi.org/10.1179/174328508X292973.

[15] Wang PZ, Rudert V, Lang E. Einfluß des TiO_2-Gehaltes auf die Reaktivität von Hüttensanden, Cem. Int. 2002;1:120–128.

[16] Wolter A, Frischat GH, Olbrich E. Investigation of granulated blast furnace slag (GBFS) reactivity by SNMS. 11th International Congress on the Chemistry of Cement Proceedings, Durban. 2003;1866-1877.

[17] Smolczyk HG. Slag structure and identification of slags. in: 7th International Congress on the Chemistry of Cement Proceedings, Paris. 1980;1:3-17.

[18] Brunelot R. Utilisation du laitier de Haut Fourneau et de la scorie LD. Commission des Communautés Européennes. 1988.

[19] Demoulian E, Gourdin P, Hawthorne F, Vernet C. Influence de la composition chimique et de la texture des laitiers sur leur hydraulicité, In: 7th International Congress on the Chemistry of Cement Proceedings, Paris.1980;2:89-94.

[20] Eaton GR, Eaton SS, Barr DP, Weber RT. Quantitative EPR. Springer Science & Business Media. 2010. https://doi.org/10.1007/978-3-211-92948-3.

[21] Ravel B, Newville M. ATHENA, ARTEMIS, HEPHAESTUS: data analysis for X-ray absorption spectroscopy using IFEFFIT. J. Synchrotron Radiat. 2005;12:537–541. https://doi.org/10.1107/S0909049505012719.

[22] Cormier L, Gaskell PH, Calas G, Soper AK. Medium-range order around titanium in a silicate glass studied by neutron diffraction with isotopic substitution. Phys. Rev. B. 1998;5:11322–11330. https://doi.org/10.1103/PhysRevB.58.11322.

[23] Iwamoto N, Hidaka H, Makino Y. State of Ti^{3+} ion and Ti^{3+}-Ti^{4+} redox reaction in reduced sodium silicate glasses. J. Non-Cryst. Solids. 1983;58:131–141. https://doi.org/10.1016/0022- 3093(83)90108-4.

[24] Jonczy I. Forms of occurrence of selected alloying elements in slag from an electric arc furnace. IOP Conf. Ser.: Earth Environ. Sci. 2019; 261:012017. https://doi.org/10.1088/1755-1315/261/1/012017.

[25] Farges F, Brown GE, Jr., Navrotsky A, Gan H, Rehr JJ. Coordination chemistry of Ti (IV) in silicate glasses and melts: II. Glasses at ambient temperature and pressure.Geochim. Cosmochim. Acta. 1996;60:3039–3053. https://doi.org/10.1016/0016-7037(96)00145-7.

[26] Farges F, Brown GE, Rehr JJ, Coordination chemistry of Ti (IV) in silicate glasses and melts: I. XAFS study of titanium coordination in oxide model compounds. Geochim. Cosmochim. Acta. 1996;60:3023–3038. https://doi.org/10.1016/0016-7037(96)00144-5.

[27] Henderson G, Liu X, Fleet M. A Ti L-edge X-ray absorption study of Ti-silicate glasses. Phys. Chem. Miner. 2002;29:32–42. https://doi.org/10.1007/s002690100208.

[28] Zheng K, Liao J, Wang X, Zhang Z. Raman spectroscopic study of the structural properties of CaO-MgO-SiO_2-TiO_2 slags. J. Non-Cryst. Solids. 2013;376:209–215. https://doi.org/10.1016/j.jnoncrysol.2013.06.003.

[29] Duan RG, Liang KM, Gu SR. The effect of Ti^{4+} on the site of Al^{3+} in the structure of CaO–Al_2O_3– SiO_2–TiO_2 system glass. Mater. Sci. Eng. A. 1998; 249:217–222. https://doi.org/10.1016/S0921-5093(98)00570-X.

[30] Burns RG, Mineralogical Applications of Crystal Field Theory.Cambridge Univ. Press, Cambridge, 1993. DOI: https://doi.org/10.1017/CBO9780511524899.022.

[31] Galoisy L, Cormier L, Rossano S, et al. Cationic ordering in oxide glasses: the example of transition elements. Mineral. Mag. 2000; 64:409-424. https://doi.org/10.1180/002646100549472.

[32] Calas G, Cormier L, Galoisy L, Jollivet P. Structure– property relationships in multicomponent oxide glasses. C. R. Chim. 2002;5:831–843. https://doi.org/10.1016/S1631- 0748(02)01459-5.

[33] Cormier L, Ghaleb D, Delaye JM, Calas G. Competition for charge compensation in borosilicate glasses: Wide-angle x-ray scattering and molecular dynamics calculations. Phys. Rev. B. 2000; 61:14495. https://doi.org/10.1103/PhysRevB.61.14495.

[34] Lee SK, Sung S. The effect of network-modifying cations on the structure and disorder in peralkaline Ca–Na aluminosilicate glasses: O-17 3QMAS NMR study. Chem. Geol. 2008;256:326– 333. https://doi.org/10.1016/j.chemgeo.2008.07.019.

[35] Bunker BC. Molecular mechanisms for corrosion of silica and silicate glasses. J. Non-Cryst. Solids. 1994;179:300–308. https://doi.org/10.1016/0022-3093(94)90708-0.

[36] Keeley P, Rowson N, Johnson T, Deegan D. The effect of the extent of polymerisation of a slag structure on the strength of alkali-activated slag binders. Int. J. Miner. Process. 2017;164:37–44. https://doi.org/10.1016/j.minpro.2017.05.007.

[37] Greaves GN. EXAFS and the structure of glass. J. Non-Cryst. Solids. 1985;71: 203–217. https://doi.org/10.1016/0022-3093(85)90289-3.

[38] Roskosz M, Toplis MJ, Richet P. The Structural Role of Ti in Aluminosilicate Liquids in the Glass Transition Range: Insights from Heart Capacity and Shear Viscosity Measurements. Geochim. Cosmochim. Acta. 2004;68:591–606. https://doi.org/10.1016/S0016-7037(03)00481-2.

[39] Romano C, Paris E, Poe BT, Giuli G, Dingwell DB, Mottana A. Effect of aluminum on Ti- coordination in silicate glasses: A XANES study. Am. Mineral. 2000;85:108-117. https://doi.org/10.2138/am-2000-0112.

[40] Bergeron B, Galoisy L, Jollivet P, et al. First investigations of the influence of IVB elements (Ti, Zr, and Hf) on the chemical durability of soda- lime borosilicate glasses. J. Non-Cryst. Solids. 2010;356:2315–2322. https://doi.org/10.1016/j.jnoncrysol.2010.07.065.

[41] Wallenberger F, Watson J, Li H. Glass Fibers. In ASM Handbook, vol. 21–Composites. Miracle, D.B. and Donaldson, S.L. Eds.; ASM International: Geauga, OH, USA, 2001.

[42] Babu MM, Prasad PS, Venkateswara Rao P, et al.Titanium incorporated zinc-phosphate bioactive glasses for bone tissue repair and regeneration : impact of Ti^{4+}on physico-mechanical and in vitro bioactivity. Ceram. Int. 2019;45:23715-23727. https://doi.org/10.1016/j.ceramint.2019.08.087.

Table 1: Composition (in wt.%) of the granulated blast-furnace slag samples obtained by X-ray fluorescence measurements. #1 concerns the specifications defined by the norm NF EN 15167-1. #2 corresponds to the usual values adopted, according to practice.

Element	**Slag 1**	**Slag 2**	**Slag 3**	**Slag 4**	**Slag 5**	**Slag 6**	**#1**	**#2**
SiO_2	39.25	36.76	35.79	37.09	36.91	35.55	-	
Al_2O_3	9.97	11.37	11.32	10.54	11.86	10.77	-	
Fe_2O_3	1.35	0.40	1.06	0.39	0.37	0.90	-	
CaO	38.52	43.31	41.62	41.24	42.13	40.94	-	
MgO	8.80	6.26	6.35	6.38	6.45	7.42	≤ 18	
SO_3	0.14	0.12	1.85	2.08	n.d.	1.68	≤ 2.5	
Na_2O	0.52	0.36	0.27	0.31	0.14	0.22	-	
K_2O	0.60	0.50	0.44	0.43	0.54	0.38	-	
TiO_2	0.49	0.58	0.94	1.21	1.34	1.86	-	
Mn_2O_3	0.33	0.3	0.32	0.34	0.25	0.27	-	
Total	**99.97**	**99.96**	**99.96**	**100**	**99.99**	**99.99**		
Glass content (*)	>95	>95	>95	>95	>95	>95		>90
C/S	0.98	1.18	1.16	1.11	1.14	1.15		>1
(C+M)/S	1.21	1.35	1.34	1.28	1.32	1.36	≥1	≥1
(C+M)/(S+A)	0.96	1.03	1.02	1.00	1.00	1.04		>1
C+M+S	84.99	87.33	85.05	84.87	83.22	84.89	> 66	
Hydraulic index	1.44	1.59	1.59	1.51	1.57	1.61		>1
Tetmayer modulus	1.54	1.70	1.70	1.62	1.67	1.73		>1

(#1): Specification according to NF EN 15167-1

(#2): Usual values according to practice

(*): Checked by XRD and birefringence

Hydraulic index = $[CaO+(1.4*MgO)+(0.56*Al_2O_3)]/SiO_2$

Tetmayer index = $[CaO/56+MgO/40+Al_2O_3/102]/[SiO_2/60]$

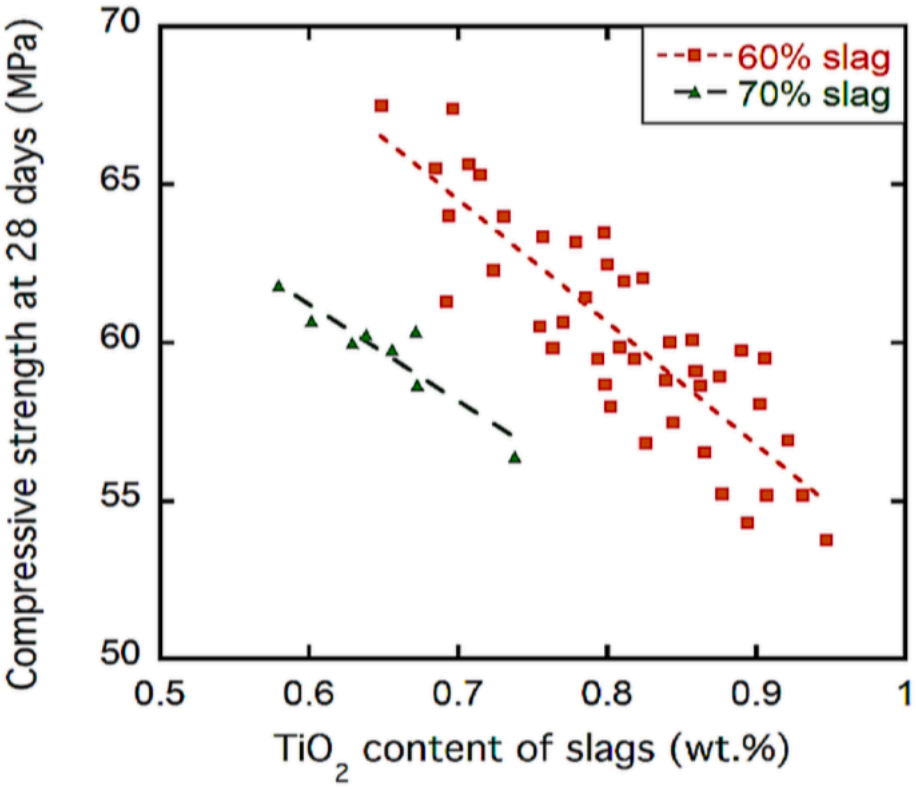

Figure 1: Evolution of the compressive strength at 28 days of mortars based on slag cements (containing 60% and 70% amorphous slag) as a function of the TiO_2 content of the slag, following the norm NF EN 196-1 (see text). The samples are representative of major European industrial plants (ATILH, pers. comm.).

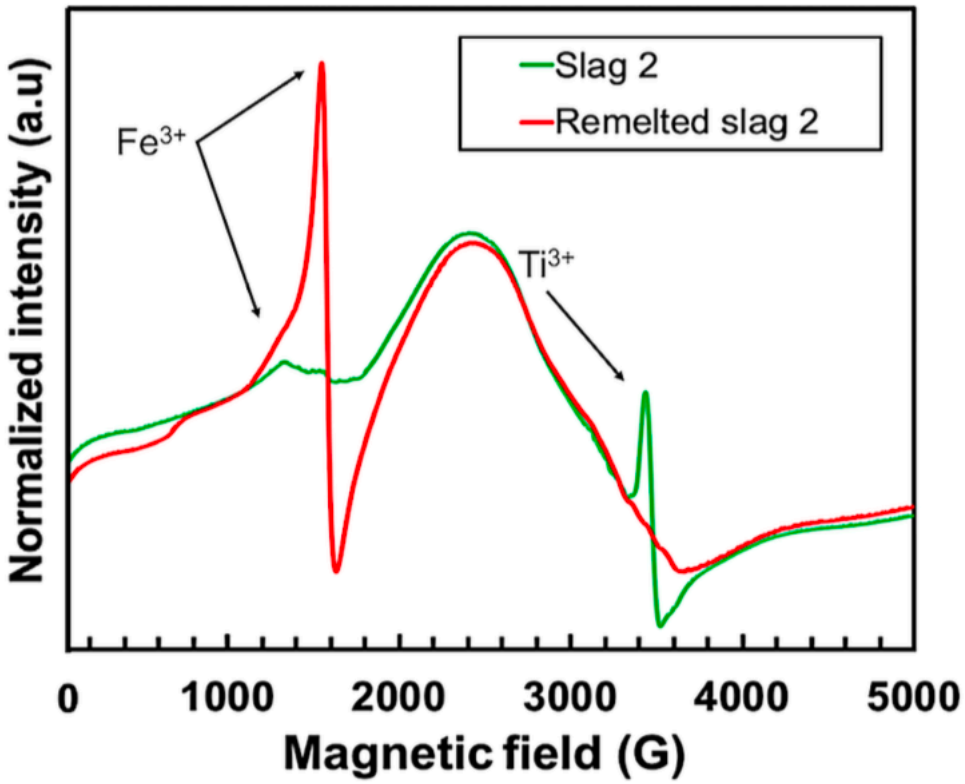

Figure 2: Electron Paramagnetic Resonance spectra of pristine and remelted slag 2. The Ti^{3+} EPR signal at near 3500G disappears after remelting under oxidizing conditions, showing the complete oxidation of Ti^{3+} into Ti^{4+}. After remelting under oxidizing conditions, some Fe^{2+} initially present in the slag is oxidized into Fe^{3+}. The large resonance centered around 2500G corresponds to magnetic clusters, probably the RO phase, unaffected by remelting.

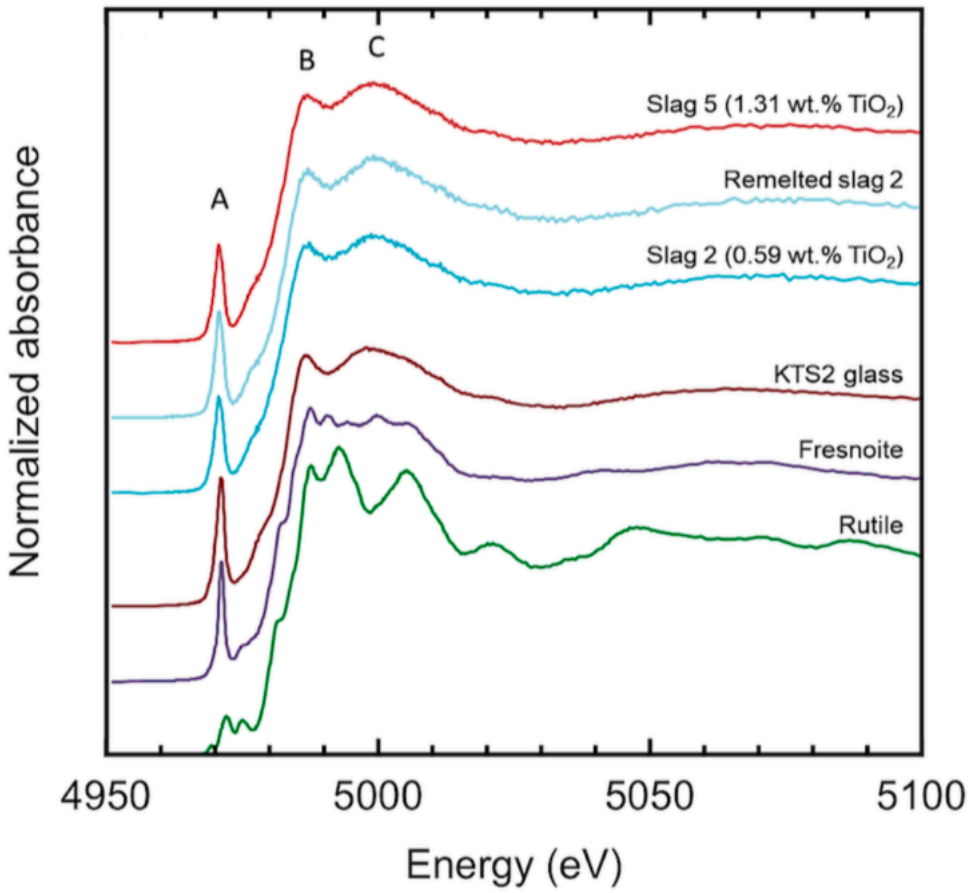

Figure 3: Ti K-edge X-ray Absorption Near-Edge Structure spectra of slags and reference samples. The spectra have been normalized to the atomic absorption. The pre-edge is the intense feature located on the low-energy side of the absorption edge.

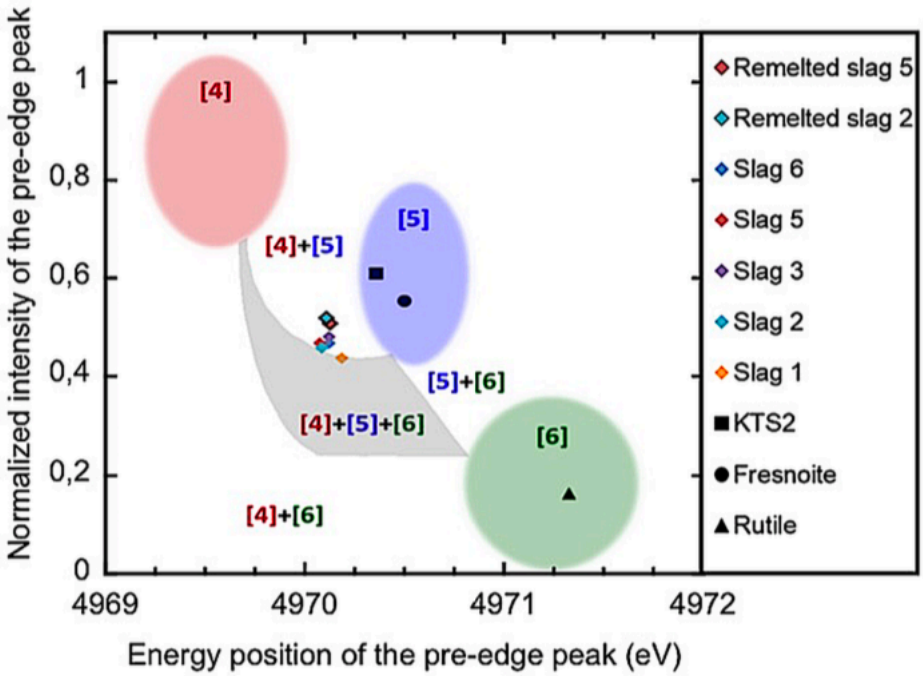

Figure 4: Energy position and normalized intensity of the pre-edge feature of the Ti K-edge XANES spectra of slags, relative to the values observed for 4-, 5- and 6-coordinated Ti (after ref. 26). The accuracy is 0.1 eV for the energy position and 0.03 for the pre-edge intensity.

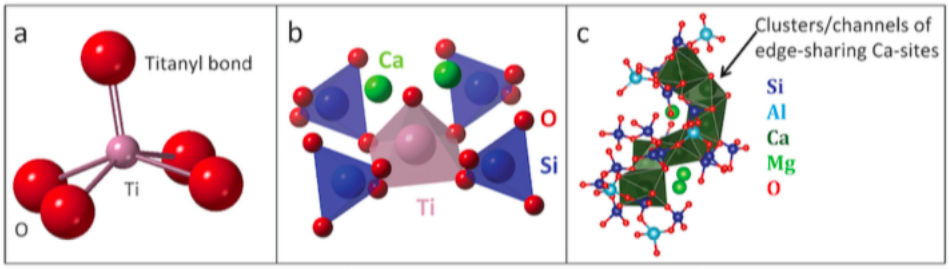

Figure 5: Illustrative representation of the local environment around Ti in slags. (a) The nearest neighbors: five- coordinated Ti^{4+} in a square pyramid geometry, showing the characteristic short Ti=O titanyl bond. (b) The next-nearest neighbors: linkage of 5-coordinated Ti to the silicate framework through Ti-O –Si bonds while the non- bonding oxygen of the short Ti=O titanyl bond requires a local charge compensation by Ca^{2+} ions. (c) Illustrative snapshot of a numerical model by Molecular Dynamics combined with Reverse Monte Carlo (Le Cornec et al., submitted) showing the atomic scale organization of Ca-sites in clusters. These clusters may represent possible pathways during glass dissolution. In these clusters, some Ca-sites may be implied in the charge compensation required by the presence of 5-coordinated Ti in their vicinity (not depicted, due to their low concentration) affecting glass reactivity.

SUPPLEMENTARY INFORMATION

S1. Experimental conditions for acquisition and treatment of the Ti K-edge XANES spectra

The storage ring of the SOLEIL synchrotron was operating at 2.75 GeV with an average current of 450 mA. The energy was calibrated using a Ti foil (first inflexion point of the pre-edge at 4966.0 eV). The spectra were recorded using from 4920 eV to 5200 eV with the following energy steps: from 4920 to 4960 eV, 2 eV/step; from 4962 to 4978 eV (pre-edge region), 0.1 eV/step; from 4978.1 to 5015 eV (edge region), 0.2 eV/step; from 5015.2 to 5050 eV, 0.5 eV/step and from 5050.5 to 5200 eV, 1 eV/step. A counting time of 1 to 3 s was chosen depending on the amount of Ti in the sample. The detector was a mono-element Si drift diode located at 90° from the incident X-ray beam direction. Sample holders were tilted so that the incident beam intersects their surfaces with a 10° angle. For each sample, three spectra were recorded and averaged.

The fluorescence signal was corrected from the dead time of the detector and normalized by the intensity of the incident signal I_0. For the reference samples that contain high amounts of Ti, self-absorption was corrected with the same software. The crystalline references, rutile and fresnoite, were checked by X-ray diffraction using the Cu K_α radiation of a PANalytical X'Pert Pro diffractometer. As the pre-edge of the rutile spectrum is composed of three components, three Lorentzian functions were used instead of one. The intensity and energy position of the second peak are the most sensitive to Ti-site geometry [24] and were used as $^{[6]}Ti^{4+}$ standard.

Figure S1. Detail of the EPR spectrum of Ti3+ in slag 6, showing the absence of isolated paramagnetic Mn2+.

Figure S2. Derivation of the Ti^{3+} content of the slag, as a function of the total Ti content (mol/g). The dotted line is a linear regression of the experimental data.

Figure S3. (a) Pre-edge features A of ground slags 1, 2, 3, 5 and 6 and KTS2 glass reference sample. (b) Pre-edge peak features A of slag 2 and remelted slag 2.